

Recovering classical dynamics from coupled quantum systems through continuous measurement

Shohini Ghose, Paul Alsing, and Ivan Deutsch

Department of Physics and Astronomy, University of New Mexico, Albuquerque, New Mexico 87131

Tanmoy Bhattacharya, Salman Habib, and Kurt Jacobs^y

T-8 Theoretical Division, MS B285, Los Alamos National Laboratory, Los Alamos, New Mexico 87545

(Dated: October 22, 2019)

We study the role of continuous measurement in the quantum to classical transition for a system with coupled internal (spin) and external (motional) degrees of freedom. Even when the measured motional degree of freedom can be treated classically, entanglement between spin and motion causes strong measurement backaction on the quantum spin subsystem so that classical trajectories are not recovered in this mixed quantum-classical regime. The measurement can extract localized quantum trajectories that behave classically only when the internal action also becomes large relative to \hbar .

PACS numbers: 03.65.Yz, 05.60.Gg, 03.65.Jd

Quantum and classical mechanics offer differing predictions for the dynamics of a closed system specified by a given Hamiltonian. In recent years, it has been widely appreciated that emergent classical behavior can arise when the quantum system is weakly coupled to an environment. Two levels of description have been used to discuss this behavior. The first utilizes the decoherence resulting from tracing over the environment to suppress quantum interference. In many circumstances this can lead to an effectively classical evolution of a phase space distribution function [1]. A more refined description is achieved when the environment is taken to be a meter that is continuously monitored, leading to a ‘quantum trajectory unraveling’ of the system density operator conditioned on the measurement record [2]. If one averages over all possible measurement results, the description reverts to that at the level of phase space distributions.

Though consistent with decoherence, the quantum trajectory approach is a powerful tool for understanding and quantitatively identifying the quantum-classical boundary [3, 4]. Continuous measurement provides information about the state of the system and thus localizes it in phase space. These localized trajectories have added quantum noise, however, due to quantum measurement backaction. Therefore, in order to recover the desired classical trajectories, the system must be in a regime where the measurement causes strong localization but weak noise. The conditions for which both constraints are satisfied determines a system action scale for which classical dynamics can be observed in trajectories. For a system with one motional degree of freedom, the required inequalities were derived in Ref. [4]. Beyond its abstract description, the trajectory approach gives a description of experiments [5] where a single quantum system is continuously monitored, making it possible to directly explore the effect of quantum backaction and the transition to classical dynamics in the laboratory. Such measurement records can be employed in real-time feedback loops open-

ing up a new regime of quantum control [6].

In this Letter we report on the emergence of classical behavior through continuous measurement of a system with more than one degree of freedom. As the number of dynamical variables are enlarged, analyzing the quantum-classical transition becomes significantly more complex. Multiple coupled degrees of freedom can possess characteristic actions that vary widely for each of them. Continuous measurement may be performed on any subset of the system variables with differing effects of quantum backaction. Finally, the quantum state of the coupled system generally becomes highly entangled so that the quantum backaction can be nontrivially distributed among the various sub-systems.

We present here the effect of continuous measurement on the dynamics of a particle with coupled spin and motional degrees of freedom. Numerical and analytical results demonstrate that even if the measured position lies in the classical regime, its entanglement with a quantum spin will result in large measurement backaction. Such a mixed quantum-classical description of systems with two coupled degrees of freedom is relevant in a variety of settings including the Born-Oppenheimer description of molecules, polaron dynamics in condensed matter [7] and the transport of ultra-cold atoms in magneto-optic traps [8]. The last case is an experimentally clean system in which state preparation, manipulation and measurement has been demonstrated [8, 9]. In this system, the coupling between the motion of the atom in the lattice and its internal spin dynamics leads to entanglement at the quantum level and chaos in the classical description [10]. Though not restricted to this system, our analysis here is motivated by these experiments.

We take as our model Hamiltonian,

$$H = \frac{p^2}{2m} + \frac{1}{2}m!z^2 + b_z J_z; \quad (1)$$

which describes a harmonic oscillator with mass m and

angular frequency ω with an additional spin (J_z) dependent constant force bJ_z , that can be interpreted as arising from a magnetic field with uniform gradient. The Hamiltonian approximates a single lattice site of a 1-D ‘‘line-angle-line’’ optical lattice [8], where z and p are the center of mass position and momentum of the atom. The spin J_z is a constant of motion and determines the effective potential seen by the center-of-mass motion: in the quantum case, eigenstates with $J_z = M_J$ see a harmonic well centered at $(M_J = jJ_z)z$ with $z = bJ_z/m!^2$. The classical analog is obtained by replacing the spin with a magnetic moment of the same magnitude [10].

The system considered here is linear, and hence, the expectation values of the Heisenberg equations of motion are exactly the classical equations, as are the equations which govern the variances. The quantum nature, however, manifests itself due to two reasons. First, the measurement backaction is a large effect on the dynamics of the quantum subsystem. Second, the classical and quantum equations of motion for the higher cumulants differ, and because of the severe quantization effects at such small actions, the distribution is far from normal. When the coupling allows the quantum subsystem to affect the classical one significantly, this non-Gaussian nature is apparent also in the latter. Measurement noise then affects a spread of the quantum state and great disparities appear between the individual trajectories.

The evolution of the system conditioned on a record of the atom’s mean position, $\hbar z_i + (8k)^{1/2} dW = dt$, is studied using a stochastic Schrödinger equation [11],

$$\begin{aligned} \tilde{d}^E &= \frac{1}{i\hbar} H - k z^2 dt + \\ &\quad \frac{p}{4k\hbar z dt} + \frac{\sigma}{2k dW} z^{\sim}; \quad (2) \end{aligned}$$

where the tilde denotes an unnormalized quantum state, k is the ‘‘measurement strength’’, and dW describes a Wiener noise process. Here we have assumed perfect measurement efficiency. Rewriting Eq. (2) in terms of POVMs [12], we can numerically evolve this equation using a Milstein algorithm for the stochastic term. We pick as our initial condition a product of minimum uncertainty coherent states in position and spin, and compare to the classical trajectories centered at the same initial points; we choose the initial spin coherent state in the x -direction. We set $b = m!^2 z = J$ with $z = 15z_g$ where z_g is the ground state root-mean-square (RMS) width of the wells. We choose $I = 1000\hbar$ and a measurement strength $k = \sigma^2 = 2z_g^2$ sufficient to observe classical dynamics of the positional degree of freedom uncoupled from the spin subsystem [4].

Consider the behavior for the smallest spin system, $J = 1/2$. We see in Fig. 1a that the quantum trajectory quickly diverges from the classical trajectory. This can be understood by noting that the initial spin state pointing in the x -direction is an equal superposition of spin-up and

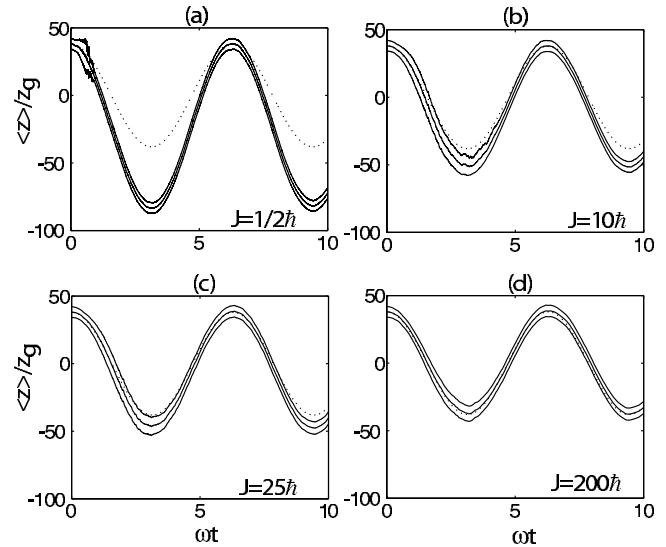


FIG. 1: Mean position of the measured system (solid) for different values of spin with $z = 15z_g$, $I = 1000\hbar$, $k = \sigma^2 = 2z_g^2$. Outer solid curves show the variance of the wave function. As J gets larger the mean position approaches the classical (dotted) trajectory.

spin-down states that move along the wells centered at $z_+ = z$ and $z_- = -z$ respectively (Fig. 2a,b). The two spin components of the initial spatially localized wave packet thus separate into a left and a right wavepacket, so that the total wave function evolves into an entangled Bell-like state, $j_L(t)i = j_L j_L^\dagger i + j_R j_R^\dagger i$, with j_L, j_R rapidly decreasing from unity. As the two components $_L$ and $_R$ see different potentials, this splitting of the wave packet is reflected in an initial rapid increase of the variance in position of the wave function (outer solid curves in Fig. 1a). Eventually, these components become resolvable beyond measurement errors, and the wave function ‘collapses’ due to the measurement into one of the wells. This contrasts the fully classical dynamics, which predicts that the spin processes freely, and the particle feels the average of the ‘left’ and ‘right’ potentials.

Unlike the spin $1/2$ case, for a large J , an initial spin coherent state in the x -direction is no longer a superposition solely of spin up and down states in the J_z basis, but rather, a distribution over all $2J + 1$ M_J states, peaked at $M_J = 0$. Just as in the spin $1/2$ case, an initially localized wave function will spread out in space as the different spinor components move along the different potentials centered at $z_{M_J} = (M_J = J)z$, (Fig. 2c,d). However, as J becomes larger, the population distribution becomes more peaked at the $M_J = 0$ state and the potentials seen by the different components are more similar. Most of the population moves along the potential centered near $z_0 = 0$, which corresponds to the classical potential. The measurement is thus more likely to localize the atom in this classical potential and damp out

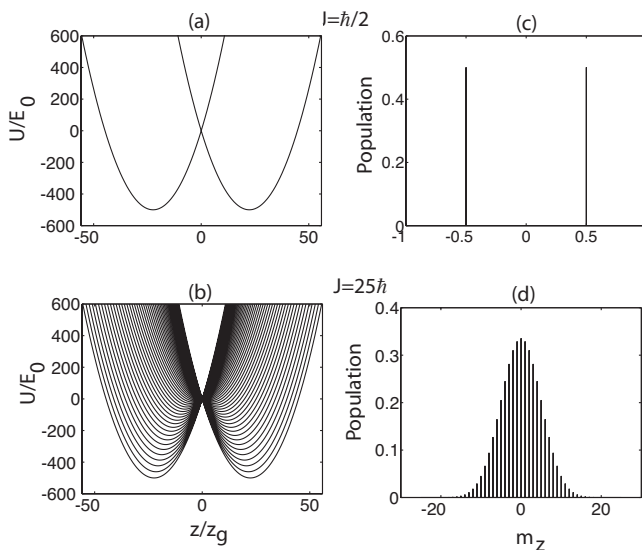


FIG. 2: The spin up and down components of a spin 1/2 wave function move along 2 different potential wells (a). For $J = 1/2$, the spin components of the wave function evolve along $2J + 1$ different potentials (b). Histograms for the populations in each m_z state for a spin-coherent state in the x -direction (c,d) show that as J gets larger the population becomes peaked around the $m_z = 0$ state. The position is thus more likely to localize the wave function in the central (classical) potential well.

the tails of the wave function that spread out over the outermost potentials. The key point is that position measurement no longer results in a strongly projective spin measurement, and therefore the weak noise condition can be met along with the strong localization condition.

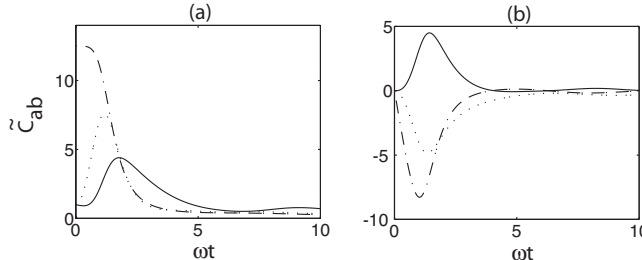


FIG. 3: Solutions of $C(t)$ for $J = 25h$ and z , I and k chosen to be the same as Fig. (1): (a) variances, $C_{zz} = z_g^2$ (solid), $C_{pp} = p_g^2$ (dotted) and $C_{zJz} = h^2$ (dashed-dotted), and (b) covariances $C_{zp} = z_g p_g$ (solid), $C_{zJz} = h z_g$ (dotted) and $C_{pJz} = h p_g$ (dashed-dotted).

We can determine analytically the scale of J for which the weak noise and strong localization conditions are satisfied by following the approach in [4]. The stochastic equations of motion for the mean position and momentum follow from Eq. (2),

$$dh_{zi} = \frac{h_{pi}}{m} dt + \frac{p}{8kC_{zz}} dW ;$$

$$dh_{pi} = \frac{m!^2 h_{zidt}}{m} + \frac{p}{8kC_{zp}} dW ; \quad (3)$$

$$dh_{Jzi} = \frac{p}{8kC_{zJz}} dW ;$$

where $C_{ab} = (h_{abi} + h_{bai})/2$ are the symmetrized covariances. The small noise and strong localization conditions applied to these equations can be combined into the condition that the covariance matrix in the basis $z; p; J_z$, remain small at all times relative to the allowed phase space of the dynamics. Here we have ignored the x and y components of the angular momentum since we are interested in measuring the position of the particle, which depends only on J_z . To determine the evolution of the covariance matrix $C(t)$, we neglect third and higher cumulants since these remain small as J becomes large. Under this approximation, the covariance matrix evolves according to a matrix Riccati equation,

$$G(t) = + C(t) C(t) + C(t) C(t)^T, \text{ where}$$

$$\begin{aligned} 0 & \quad 1 & \quad 0 & \quad 1 \\ 0 & \quad 0 & \quad 0 & \quad 8k \quad 0 \quad 0 \\ = & @ 0 \quad 2h^2 k \quad 0 A ; & = & @ 0 \quad 0 \quad 0 A ; \\ 0 & \quad 0 & \quad 0 & \quad 0 \quad 0 \quad 0 \\ 0 & \quad 0 & \quad 1 = m & \quad 0 & \quad 1 \\ = & @ m!^2 \quad 0 & \quad m!^2 z A : & & \\ 0 & \quad 0 & \quad 0 & & \end{aligned} \quad (4)$$

Since the matrices C , C_{zz} , and C_{pp} are time independent, it is possible to analytically solve this equation [13]. Furthermore, when the external action becomes very large ($h \neq 0$), can be neglected and the solution $C(t)$ is easily determined. Even under this approximation, the analytical solutions for the second cumulants are in general not simple functions of the system parameters. We resort to a numerical calculation to find the bounds on the analytical solutions $C(t)$. Our studies indicate that the bounds on $C(t)$ decrease as J is increased, as expected. Fig. 3 shows a typical plot of $C(t)$ with $J = 25h$ and $I = 1000h$. For this value of J , the maximum variance in the measured position is already smaller than the allowed phase space of the dynamics (Fig. 1c) by a factor about 50.

Our numerical and analytical results show that classical dynamics is only recovered in this coupled system when the actions of both subsystems become large relative to h . When one subsystem lies in the quantum regime, even a weak measurement of the classical subsystem eventually results in a strongly projective measurement of the quantum subsystem, thus preventing the recovery of classical behavior. The dynamics of such coupled systems has previously been approximated in other contexts using a mixed quantum-classical description [14], where the classical subsystem variables are described by numbers while the quantum subsystem variables are treated as quantum mechanical operators. Such a description results in equations of motion for them that can lead to chaotic dynamics when an additional transverse magnetic field is applied. However, in the absence of an appropriate separation of time scales, the

prediction of chaos arising from such a mixed quantum-classical description has been shown to fail [15]. Here we find that even in a regular non-chaotic regime, for open systems this mixed quantum-classical description would have limited validity since it does not take into account the effect of measurement backaction when the system is actually observed. While the Hamiltonian and Heisenberg equations of motion will certainly agree in the ensemble mean, variances will be quite large so that the measured individual quantum trajectories will diverge strongly from the mean. The same argument should hold for open systems in the chaotic regime.

We have focused so far on recovering the classical dynamics of the measured quantity, here the position of the atom. One may also ask whether the internal degree of freedom follows the classical trajectory. We find that classically, for a perfectly defined initial condition, the magnetic moment precesses in the x-y plane forever. Quantum mechanically, however, since the position measurement in our example only localizes the z-component of the spin, the x and y components of the spin are not localized. Since the uncertainty principle allows a perfect knowledge of the z-component only if the x- and y-components have zero average, in the long time limit these dephase to zero. A position measurement would localize the wave function in all spin directions had we added a coupling magnetic field in the x-y direction that acts to mix the different components. On the other hand, a fair comparison between the quantum and classical dynamics would be to choose a classical probability distribution of initial points, consistent with the quantum spin coherent state. Such a classical system does dephase over time.

Beyond the behavior of the observables of each marginal subsystem (internal and external), entanglement in the whole system characterizes the quantum to classical transition. In the spin-1/2 case we have seen that the state can develop nearly maximal entanglement, when the spin-up and spin-down wavepackets become spatially resolved. For larger values of J , the evolution never results in such resolution, and hence, the entanglement, which is determined by the overlap between the different spinor components of the wave function, also decreases as J increases. For pure bipartite systems, the entanglement is given by the von Neumann entropy of the marginal density matrix \sim for either subsystem, $E = -\text{Tr}(\sim \ln \sim)$. The degree of entanglement generated in stochastic dynamics can be compared for different values of J by calculating the normalized value, $E_{\text{max}} = E_{\text{max}}/E_0$, where E_{max} is the maximum entropy achieved during the monitored evolution and E_0 is the maximum possible entropy for the chosen initial state. We find that E_{max} falls off with J as expected, and with a $1=J$ dependence for large J . These results raise intriguing questions about the role of entanglement between subsystems in the transition to classical behavior.

In future work we hope to investigate these issues further. Our model Hamiltonian becomes non-integrable when an additional magnetic field in the x-direction is applied. We propose to generalize our results to this non-integrable regime and study the emergence of classical chaos through continuous measurement and decoherence.

We thank Poul Jessen and Daniel Steck for helpful discussions. SG, PMA and IH D were supported under NSF Grant No. PHY-009569.

Electronic address: sghose1@unm.edu
 y Present Address: Arabelle SA, 69 Rue de Paris, 91400, Orsay, France

- [1] S. Habib, K. Shizume, and W. H. Zurek, *Phys. Rev. Lett.* 80, 4361 (1998).
- [2] H. Carmichael, *An Open System Approach to Quantum Optics* (Springer-Verlag, Berlin, 1993).
- [3] T. P. Spiller and J. F. Ralph, *Phys. Lett. A* 194, 235 (1994); M. Schlauder and R. Graham, *Phys. Rev. E* 52, 340 (1995); T. Brun, I. Percival, and R. Schack, *J. Phys. A* 29, 2077 (1996).
- [4] T. Bhattacharya, S. Habib, and K. Jacobs, *Phys. Rev. Lett.* 85, 4852 (2000).
- [5] H. Mabuchi, J. Ye, and H. J. Kimble, *Appl. Phys. B* 68, 1095 (1999); P. W.arszawski, H. M. Wiseman, and H. Mabuchi, *Phys. Rev. A* 65, 023802 (2001).
- [6] H. M. Wiseman, *Phys. Rev. A* 49, 2133 (1994); A. C. Doherty, S. Habib, K. Jacobs, H. Mabuchi, and S. M. Tan, *Phys. Rev. A* 62, 012105 (2000).
- [7] D. Hennig and B. Esser, *Phys. Rev. A* 46, 4569 (1992); T. Holstein, *Ann. Phys.* 8, 325 (1959).
- [8] I. H. Dutsch and P. S. Jessen, *Phys. Rev. A* 57, 1972 (1998).
- [9] D. L. Haycock, P. M. Alsing, I. H. Dutsch, J. G. Rondal斯基, and P. S. Jessen, *Phys. Rev. Lett.* 85, 3365 (2000).
- [10] I. H. Dutsch, P. M. Alsing, J. G. Rondal斯基, S. Ghose, D. L. Haycock, and P. S. Jessen, *J. Opt. B: Quantum and Semiclassical Optics* 2, 633 (2000); S. Ghose, P. M. Alsing, and I. H. Dutsch, *Phys. Rev. E* 64, 056119 (2001).
- [11] G. J. Milburn, K. Jacobs, and D. F. Walls, *Phys. Rev. A* 50, 5256 (1994); A. C. Doherty and K. Jacobs, *Phys. Rev. A* 60, 2700 (1999).
- [12] C. M. Caves and G. J. Milburn, *Phys. Rev. A* 36, 5543 (1987).
- [13] W. T. Reid, *Riccati Differential Equations* (Academic Press, New York, 1972).
- [14] H. Schanz and B. Esser, *Phys. Rev. A* 55, 3375 (1997); R. Blumel and B. Esser, *Phys. Rev. Lett.* 72, 3658 (1994); P. Belobrov, G. Zaslavskii, and G. K. Tartakovskii, *Sov. Phys. JETP* 44, 945 (1976); P. W. M. iltoni, J. R. Ackerman, and H. W. Galbraith, *Phys. Rev. Lett.* 50, 966 (1983).
- [15] L. E. Ballentine, *Phys. Rev. E* 63, 056204 (2001); F. Cooper, J. Dawson, S. Habib, and R. D. Ryne, *Phys. Rev. E* 57, 1489 (1998).